Journal of Applied Biomechanics
Original Research

Is power grasping contact continuous or discrete?

Todd C. Pataky,[1] Greg P. Slota,[2] Mark L. Latash,[2] and Vladimir M. Zatsiorsky[2]

[1]Department of Bioengineering, Shinshu University, Ueda, Nagano, Japan
[2]Department of Kinesiology, The Pennsylvania State University, State College, PA, USA

Funding: JSPS Wakate B Grant #22700465, NIH grant #AR-048563.

Conflict of Interest Disclosure: The authors have no financial conflict of interest.

Corresponding Address: Todd Pataky, Department of Bioengineering, Shinshu University, Tokida 3-15-1, Ueda, Nagano, Japan

Abstract

During power grasp the number of local force maxima reflects either the central nervous system's preferential use of particular hand regions, or anatomical constraints, or both. Previously both biomdal and trimodal force maxima have been hypothesized for power grasp of a cylindrical handle. Here we measure the number of local force maxima, with a resolution of 4.8°, when performing pushing and pulling efforts in the plane perpendicular to the cylinder's long axis. Twelve participants produced external forces to eight targets. The number of contacts was defined as the number of local maxima exceeding background variance. A minimum of four and a maximum of five discrete contacts were observed in all subjects at the distal phalanges and metacarpal heads. We thus reject previous hypotheses of bimodal or trimodal force control for cylindrical power grasping. Since we presently observed only 4-5 contacts, which is rather low considering the hand's kinematic flexibility in the flexion plane, we also reject hypotheses of continuous contact, which are inherent to current grasping taxonomy. A modification to current grasping taxonomy is proposed wherein power grasp contains separate branches for continuous and discrete contacts, and where power and precision grasps are distinguished only by grasp manipulability.

***Keywords*:** precision grasp, hand and finger biomechanics, force coordination, distributed load, statistical parametric mapping

Introduction

It has long been postulated that power and precision grasp are taxonomically distinct: one adopts power grasps for security and stability, and precision grasps for dexterity and sensitivity.[1,2] Indeed the labels themselves –'power' and 'precision' – imply that the former is simpler, requiring less cognitive control, an implication supported by neurophysiological evidence of substantially more activity in higher cortical centers during precision grasp.[3] Yet, ironically, the equations defining power grasp dynamics are decidedly more complicated than those for precision grasp; whereas precision grasps can be modeled using discrete endpoint wrenches (i.e. forces and moments), power grasps also involve dynamically varying contact surfaces that may not be possible to control independently given a finite number of actuators.[4] Precision grasps, which have fewer kinematic constraints, thus have superior manipulability, and this may drive the need for increased higher-level neural activity.[3]

But what is the observable distinction between power and precision grasps? It has been asserted that one important factor distinguishing power from precision grasps is "*large areas of contact between the grasped object and the surfaces of the fingers and palm*" (p.1534).[1] This is intuitive, but has not, to our knowledge, been tested explicitly. If this assertion is correct, then all power grasps should exhibit 'large' areas of contact; for the present purposes we shall assume that 'large' implies greater than null forces, over continuous contact areas that are of the same order of magnitude as the total palmar area of the hand. If not all power grasps exhibit large areas of contact, then there are two possibilities: either (i) certain power grasps can be better classified as 'precision' or (ii) the aforementioned definition of power grasps is incorrect. In either case the

taxonomical definition of 'power grasp' would require revision. The present paper tests the assertion of "large areas of contact" for cylindrical grasping tasks.

Cylindrical grasping, a type of power grasping,[1] is commonly employed when handling every-day objects like: cups, steering wheels, door handles, levers, etc. It has been widely investigated, but many previous studies used discrete sensors[5-8] so these data are not directly useful for testing the aforementioned hypothesis of large contact areas. Of the studies which measured cylindrical force distribution with a continuous sensor grid, most had either angular resolutions that were too low, on-the-order-of 60°,[9] and were thus unable to distinguish between local vs. continuous contact, or had sufficiently high angular resolutions but failed to explicitly report standard deviations[10-12]. Thus the results of previous studies cannot be used to statistically test the hypothesis of large-contact areas.

There only two existing studies, of which we are aware, that provide data directly relevant to this issue. [13-14] The former (resolution: 18°) reports continuous force production over a broad contact region, thereby supporting the hypothesis, but also shows two local maxima in the 'radial' force distribution profile (i.e. in the plane perpendicular to the cylinder's long axis), which the authors described as a "bimodal distribution". The latter (resolution: 4.8°) reports forces concentrated at three points, henceforth a "trimodal distribution": the distal phalanges and the first metacarpal joint, with negligible forces in-between.

The distinction between large contact areas (i.e. a continuous distribution) and multimodal distributions has non-trivial implications for grasping control: unimodal and bimodal distributions imply a simple clamp-like mechanism, with one local maximum opposing movement, and a second potential local maximum closing the grasp. In contrast, tri- and higher order multi-

modal distributions indicate that several discrete parts of the hand exert force, which may imply (non-clamp-like) coordinated control.

The purpose of the present study was to test the null hypothesis – following an existing definition of 'power grasps'[1] – that power grasping involves large areas of contact whose force is greater than background noise. Based on recent evidence from relatively high resolution measurements[13] we propose the following alternative hypothesis: some types of power grasping can be characterized as a set of unconnected discrete contacts.

Methods

Subjects

Twelve right-handed male subjects (age: 32±8.1 years, height: 178.0±6.6 cm, mass: 81.5±14.8 kg, hand length: 18.6±1.0 cm, metacarpal head width: 9.0±0.6 cm) provided informed consent to participate in this experiment, following the policies of The Pennsylvania State University Institutional Review Board. None of the participants reported neurological or upper extremity pathology.

Equipment

A height-adjustable chair with two shoulder and waist straps was used to secure subjects in a controlled posture, with their upper and lower arms parallel to the horizontal (*xy*) plane, and with horizontal plane shoulder and elbow angles of zero and 90°, respectively (Fig.1). A vertically-oriented polyvinyl chloride (PVC) cylindrical handle (diameter=6 cm) was fixed to a six-axis load cell (Mini-85, ATI Industrial Automation, Apex, NC, USA). The instrumented handle was positioned in the *xy* plane with sliders to control for hand posture, with a gap between

the fingers at approximately +150° from the +*x* axis (Fig.1b). Subsequently slider screws were tightened, fixing the handle position.

A flexible pressure mat (thickness: 2 mm, sensing area: 25×25 cm) (PX200:100:100:10, XSENSOR Technology Corp., Calgary, Canada) was fixed to the PVC handle using overnight pre-dried adhesive spray (Photo Mount, 3M, St. Paul, MN, USA). The adhesive supported the pressure mat's weight, and the mat's data cables were supported by cords hung from ceiling rafters. The device was manufacturer-calibrated to a range of 1-200 kPa and had a spatial resolution of 2.54 mm, yielding an angular resolution of 4.8° when wrapped on the handle.

Force data were measured at 1000 Hz using LabView 8.2 (National Instruments, Austin, TX, USA). Pressure data were collected at 16 Hz, the device's maximum sampling frequency, using the manufacturer's software.

Task

The task was to produce a force of 30 N in one of eight directions separated by 45° in the horizontal (*xy*) plane (Fig.1b). A 30 N magnitude was chosen based on pilot studies of maximal efforts, which found that 30 N corresponded to approximately 50% of maximum effort in the direction perceived to be most difficult. This task was difficult enough that subjects had to grasp the handle firmly, but was not so demanding as to risk muscular fatigue. The eight force targets were presented in a circular arrangement on a computer display with the radius (30 N) maximized to fit the display (Fig.1b). The *xy* planar force vector acting on the handle was also presented. Subjects were instructed to: "move the force vector to the highlighted target quickly but smoothly over a period of approximately one second" and then to "hold the force vector in the target, using minimal muscular co-contraction, for another four seconds" until a computer tone

specified the end of the trial five seconds after initial target presentation. Three repetitions of each target were performed in a randomized order, yielding 24 trials per subject. Subjects were instructed to maintain a constant grasping posture between trials (20 s). A foam-covered PVC half-pipe arm-rest was suspended from rafter cables; subjects were permitted to use this arm- rest only between trials.

Data processing

The time window from 2-4 s was selected for analysis; for all trials this window was visually confirmed to both follow the initial force ramping period and precede anticipatory relaxation, if present. Both pressures and forces were averaged within this time window. From the original 2D pressure data (Fig.2a), 1D radial force distributions (units: N/rad) (Fig.2b) were computed as:

$$F_r(\theta) = \frac{A}{\Delta r} \sum_{z=0}^{Z} I(\theta, z) \qquad (1)$$

where θ is the polar angle (Fig.2), A is the area of a single sensor (6.45 mm^2), Δr is the angular resolution (0.083 rad), and $I(\theta,z)$ is the pressure recorded at the handle's (θ,z) coordinates. Thus F_r represents the total force per-angular-unit that acts at a specific location θ. The F_r distributions (Fig.2b) were then averaged within-subjects for each of the eight tasks. "Grasp force" was also computed as:

$$\text{Grasp force} \equiv \sum_{\theta=0}^{2\pi} F_r(\theta) \qquad (2)$$

Since anatomical differences amongst subjects cannot be normalized through simple hand-size scaling[13], inter-subject anatomical variability was presently normalized, as in the cited

study, as follows: first five points of interest (POI) were manually digitized on the pressure data (Fig.2a): the distal thumb phalanx - DP1, the first and second metacarpophalangeal joints - MCP1, MCP2, and the distal phalanges of index and middle fingers - DP2, DP3. Next the force distribution curves were aligned using piecewise-linear radial warping[15] amongst the five POIs.

Statistics

Radial force distributions were analyzed using Statistical Parametric Mapping (SPM).[16] Briefly, the mean radial force distribution was normalized by its degree-of-freedom-corrected variance, yielding a radial *t* distribution, or an "SPM{t}". Random field theory[17] was then used to determine the critical *t* threshold (at a specified family-wise error rate of α), above which portions of the SPM{t} were considered statistically significant. This process is analogous to univariate statistical inference, where an α threshold maps precisely to a *t* threshold given the experimental degrees of freedom. The key difference is that presently many *t* tests were conducted (specifically: one at each radial node, separated by 4.8°), and thus the probability of observing a large *t* value was higher than if only a single test had been conducted. This problem is typically handled using the Bonferroni correction for multiple comparisons, but this correction procedure is overly conservative because it fails to account for correlation amongst neighboring nodes. The random field theory correction, on the other hand, uses the gradient of the residual field to estimate the number of "resolution elements",[16] or equivalently, the number of independent processes, and then raises the critical *t* threshold accordingly to retain a constant family-wise error rate (of α).

Presently, one-sample *t* tests were conducted to determine which parts of the radial force distribution were significantly higher than null force. One test was conducted for each of the

eight task directions, and one final test was conducted for the overall mean distribution. The family-wise error rate was set at α=0.05, with a Bonferroni correction to 0.0056 to compensate for the nine separate tests. SPM analyses were conducted using 'SPM1D', an open source software package,[18] and the remainder of the analyses were conducted in Python 2.7 using the Enthought Python Distribution (Enthought Inc., Austin, TX, USA).

Local force pulse modeling

Acknowledging that soft tissue's spatial dissipation of forces under bony structures can be approximated by the Gaussian function,[19-20] we presently asked the following question: if we assume that power grasping is controlled at a number of discrete contacts, and that forces at these contact points can be modeled locally as Gaussian pulses, how much of the variability in the data can be explained by n contacts? Experimental force distributions were thus modeled as summations of n Gaussian pulses:

$$f(\theta) \equiv \sum_{t=0}^{n} a_i e^{-(\theta - b_i)^2 / 2c_i^2} \quad (3)$$

where parameters a_i, b_i, and c_i modulate pulse amplitude, position, and breadth, respectively. Analyses proceeded as follows: (i) assuming n pulses, find the optimum location b_i for each pulse using data from the average task, and then (ii) find the optimum amplitude and breadth (a_i and c_i), separately for each task. Under this scheme pulse location b_i was constant for each task, mimicking the present experiment's constant hand posture. The optimization goal was to minimize the sum-of-squared-errors between the modeled and experimental data. A hierarchical implementation[21] of particle swarm optimization[22] was used to determine the optimum values for the n×3 parameters. Following experimental observations of four-to-five pulses (Fig.2b), n

was varied between one and eight. Model fit quality was quantified by the root mean squared error. The case of the uniform distribution was also analyzed as a comparative reference.

Results

Force distributions from an example subject varied systematically amongst the eight force targets (Fig.3), with forces applied primarily to the handle opposite the target force direction, as expected. Radial forces were limited primarily to four points: DP1, DP2-3, MCP1 and MCP2.

These trends were consistent in between-subject analyses (Fig.4), with relatively small variability about the mean trend across subjects. One exception was subjects with relatively long third digits, who exhibited separate force peaks for DP2 and DP3 (Fig.2b). For all subjects a minimum of four and a maximum of five force peaks were observed. The overall mean trend (Fig.4, central panel), which is essentially a histogram summarizing radial force frequency and intensity, illustrates that DP1, DP2 and MCP2 were used most preferentially across all tasks.

SPM results confirmed the statistical significance of these mean trends, with only four clearly significant peaks across subjects (Fig.5). A potentially fifth peak between the MCP2 and DP2 locations was observed for the 135 and 225° tasks. However, force values in this region were quite low for these two tasks (Fig.4).

Since the digits did not wrap completely around the handle, subjects reported that some task directions were more difficult than others, and the 315° direction, in particular was reported to be most difficult. This qualitative observation was reflected in grasp force results (Fig.6), which showed that subjects grasped the handle most firmly for the 315° direction, and that grasp

force was asymmetrically distributed amongst the target directions. Despite qualitative difficulty differences across the tasks, the trend for four local radial force peaks (Figs.4-5), or five in the case of peculiar subjects (Fig.2b), was consistent across all tasks (Fig.5).

As in previous studies[19-20] spatial force pulse modeling was found to reproduce local loading qualitatively well (Fig.7a), but only if a suitably large number of pulses was modeled; the distinct DP2 and DP3 pulses could not be reproduced in an example subject with only three pulses (Figs.2b,7a). Indeed the fits between the modeled and experimental data improved in an exponential-like manner (Fig.7b), with the bulk of improvement achieved with only four pulses. Specifically, three and four pulses accounted for 69.9±12.4% and 81.2±3.7% greater variance (than the uniform distribution), but eight pulses improved the fit by only ~5% to 86.5±4.5%.

Discussion

It was presently shown that radial forces exerted during cylindrical grasping were significantly greater than null force only at four or five discrete regions of the hand surface: the distal phalanges and metacarpophalangeal joints (Fig.5). We thus reject the null hypothesis that all power grasping involves large areas of contact[1] whose force is greater than background noise, in favor of the alternative hypothesis: that some power grasps are more aptly characterized as a set of localized discrete contacts. Caveats to this finding are that continuous contact forces are commonly reported for maximal efforts[9,12,14] and some sub-maximal tasks[8,23], including sub-maximal pulling in the longitudinal direction[13].

The taxonomic implications are twofold (Fig.8). First, contact continuity does not distinguish power from precision grasps. Second, power grasping contact may be characterized as

either continuous, as reported or implied in previous studies[9,10,14,23], or non-continuous, as presently observed; some power grasps can be better characterized as a collection of (locally continuous) discrete contacts.

The present findings additionally have implications for our understanding of power grasp control. A preferential adoption of discrete over continuous contact could represent a strategy for avoiding the mechanical complexities of continuous contact[4] in cases where manipulability is valued. In the context of the present experimental task, discrete contact may have helped with external force direction control.

The underlying mechanisms driving discrete vs. continuous contact could be either neural, reflecting central nervous system control preferences, or anatomical, reflecting interacting anatomical and geometrical task constraints. Or the mechanisms could have both neural and anatomical underpinnings. With the present dataset we are unable to test a neural vs. anatomical hypothesis, so we propose a null hypothesis instead: discrete contacts observed during cylindrical handle power grasping arise purely from anatomical and mechanical peculiarities, and thus do not reflect active control preferences of the central nervous system. To test this hypothesis we could, for example, isolate the hand from neural feedback via rapid handle perturbations, where neural feedback loops could not act rapidly enough to affect contact area. If discrete contacts remain in this 'deafferented' case, this would provide evidence in favor of the anatomical hypothesis.

It is presently unclear why previous studies failed to elucidate discrete contacts during power grasp. We believe there are potentially three explanations. First, spatial resolutions were generally lower in previous studies, so it may not have been possible to accurately characterize

signals with relatively high (radial) spatial frequency (Fig.4). Second, amongst other factors like load type and magnitude, the appearance of discrete vs. continuous contact may be dependent on handle diameter. Pilot results have shown that discrete contacts may fuse into contacts that can be better described as 'continuous' as the handle diameter reduces; however, this requires systematic exploration to be conclusive.

Third, many previous studies investigated maximal grasp,[9,14] while the current task was, at 30 N, decidedly sub- maximal; nevertheless power and precision grasp are not distinguished based on intensity. Lastly, most previous studies reported discrete rather than continuous statistics; the current statistical parametric mapping (SPM) approach[16] allowed us to statistically examine the force distribution at effectively the same spatial resolution as the raw data. Without a continuous statistical approach like SPM it would not be possible to test hypotheses of continuous contact.

In summary, the present data provide strong evidence that not all power grasping can be characterized by continuous contact; in some cases, like the present cylindrical grasping with pushing and pulling forces in the normal plane, power grasping is more accurately characterized by a small set of discrete contact points at the distal phalanges an metacarpophalangeal joints. We have proposed a modified version of an established grasping taxonomy[1] which distinguishes power from precision grasp based only on the cited study's original manipulability hypothesis. We have also proposed competing neural vs. anatomical hypotheses to explain the presently observed discrete contacts. We hope that the present results can lead to a more comprehensive taxonomy of power grasp, which may be useful for both categorical programming of robotic grasp control, and for categorically focused clinical rehabilitation.

References

1. Cutkosky MR, Wright PK. Modeling manufacturing grips and correlations with the design of robotic hands, *IEEE Int Conf Robot Autom* San Francisco, CA 1986; 1533-1539.

2. Napier J. The prehensile movements of the human hand. *J Bone Joint Surg* 1956; 38B(4):902–913.

3. Ehrsson HH, Fagergren A, Jonsson T, Westling G, Johansson RS, Forssberg H. Cortical activity in precision-versus power-grip tasks: an fMRI study. *J Neurophysiol* 2000; 83(1):528–536.

4. Zhang Y, Gruver WA. Force distribution of power grasps based on the controllability of contact forces. *Conf Proc IEEE Int Conf Syst Man Cybern* 1995; 93–88.

5. Gurram R, Gouw GJ, Rakheja S. Grip pressure distribution under static and dynamic loading. *Exp Mech* 1993; 33(3):169–173.

6. Hall C. External pressure at the hand during object handling and work with tools, *Int J Ind Ergon* 1997; 20(3):191–206.

7. Kargov A, Pylatiuk C, Martin J, Schulz S, Doderlein L. A comparison of the grip force distribution in natural hands and in prosthetic hands. *Disabil Rehabil* 2004; 26(12):705–711.

8. Shimojo M, Sato S, Seki Y, Takahashi A. A system for simultaneously measuring grasping posture and pressure distribution. *IEEE Int Conf Robot Autom* 1995.

9. Wimer B, Dong RG, Welcome DE, Warren C, McDowell TW. Development of a new dynamometer for measuring grip strength applied on a cylindrical handle. *Med Eng Phys* 2009; 31:695–704.

10. Aldien Y, Welcome D, Rakheja S, Dong R, Bouileau P-E. Contact pressure distribution at hand-handle interface: role of hand forces and handle size. *Int J Ind Ergon* 2005; 35(3):267–286.

11. Lemerle P, Klinger A, Cristalli A, Geuder M. Application of pressure mapping techniques to measure push and gripping forces with precision. *Ergonomics* 2007; 51(2):168–191.

12. Seo NJ, Armstrong TJ, Ashton-Miller JA, Chaffin DB. The effect of torque direction and cylindrical handle diameter on the coupling between the hand and a cylindrical handle. *J Biomech* 2007; 40(14):3236–3243.

13. Pataky TC, Slota GP, Latash ML, Zatsiorsky VM. Radial force distribution changes associated with tangential force production in cylindrical grasping, and the importance of anatomical registration. *J Biomech* 2012; 45(2):218–224.

14. Young JG, Sackllah ME, Armstrong TJ. Force distribution at the hand/handle interface for grip and pull tasks. *Proc Hum Fact Ergon Soc Annu Meet* 2010.

15. Kneip A, Li X, MacGibbon KB. Curve registration by local regression. *Can J Stat* 2000; 28(1):19–29.

16. Friston KJ, Ashburner JT, Kiebel SJ, Nichols TE, Penny WD. *Statistical Parametric Mapping: The Analysis of Functional Brain Images*. Amsterdam: Elsevier/Academic Press; 2007.

17. Adler RJ, Taylor JE. *Random Fields and Geometry*, London: Springer; 2007.

18. Pataky TC. One-dimensional statistical parametric mapping in Python. *Comput Methods Biomech Biomed Engin* 2012; 15(3):295–301.

19. Lord M. Spatial resolution in plantar pressure measurement. *Med Eng Phys* 1997; 19(2):140–144.

20. Pataky TC. Spatial resolution in plantar pressure measurement revisited [published online ahead of print June 22, 2012]. *J Biomech* http://www.sciencedirect.com/science/article/pii/S0021929012003193

21. Ratnaweera A, Halgamuge SK, Watson HC. Self- organizing hierarchical partial swarm optimizer with time-varying acceleration coefficients. *IEEE Trans Evol Comput* 2004; 8(3):240–255.

22. Kennedy J, Eberhart RC. Particle swarm optimization, *Proc Int Jt Conf Neural Netw* 1995; 1942–1948.

23. Sinsel EW, Gloekler D, Wimer B, Warren C, Wu JZ, Buczek FL. A novel technique quantifying phalangeal interface pressures at the hand-handle interface. *Proceedings of the 34th Annual Meeting of the American Society of Biomechanics* Providence, Rhode Island 2010.

Figures

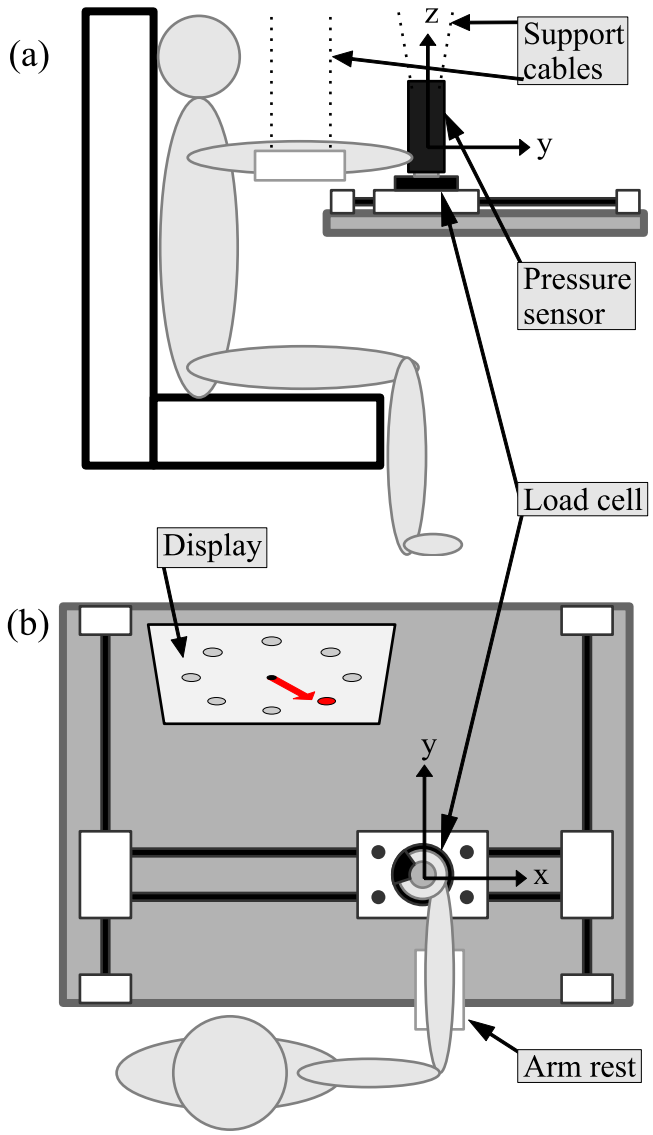

Figure 1 — Experimental apparatus, (a) side and (b) top views. The task was to produce a target force vector in the *xy* plane via visual feedback, where the display's right and up and directions corresponded to the laboratory +*x* and +*y* directions, respectively. The gap between the thumb and lateral digits was centered at +150°, as depicted.

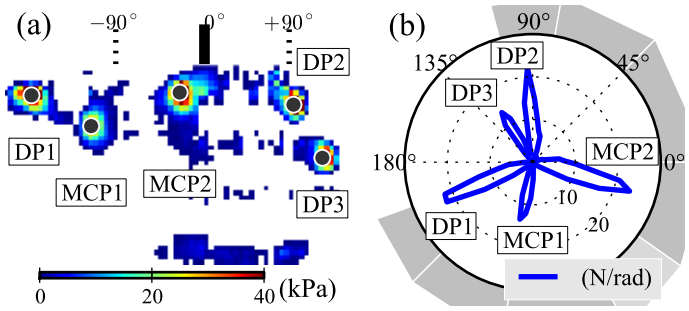

Figure 2 — Data processing overview. (a) Average pressure distribution for an example subject, across all conditions. (b) Polar force distribution, top view, with sketch depicting approximate hand posture. Five points were digitized: distal thumb phalanx - DP1, first and second metacarpophalangeal joints - MCP1, MCP2, distal phalanges of index and middle fingers - DP2, DP3.

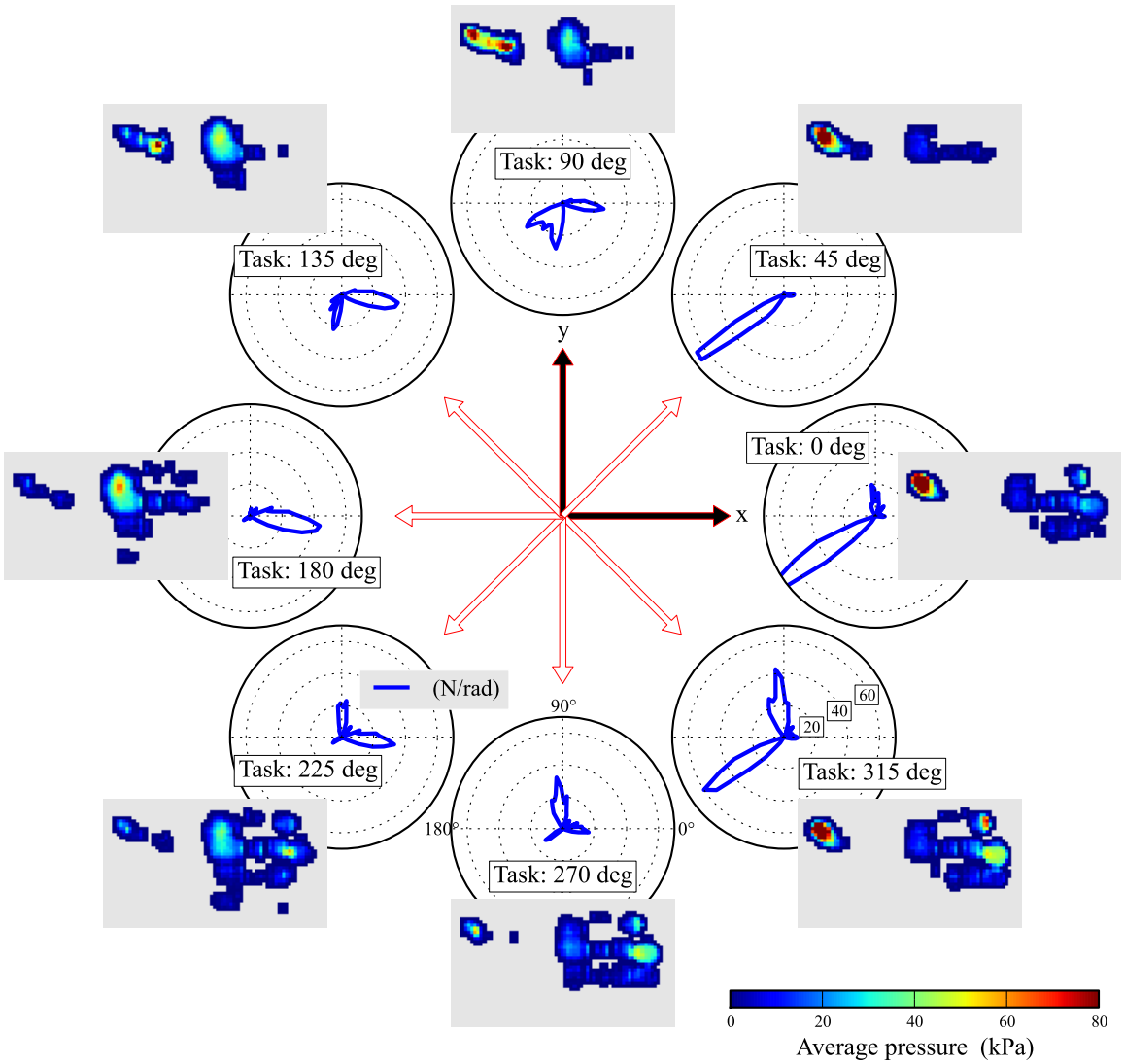

Figure 3 — Pressure and radial force distributions for an example subject, averaged across trials. Data are presented as above (Fig.2). Arrows indicate the eight target force directions in the *xy* plane. All radial force distributions have the same scale.

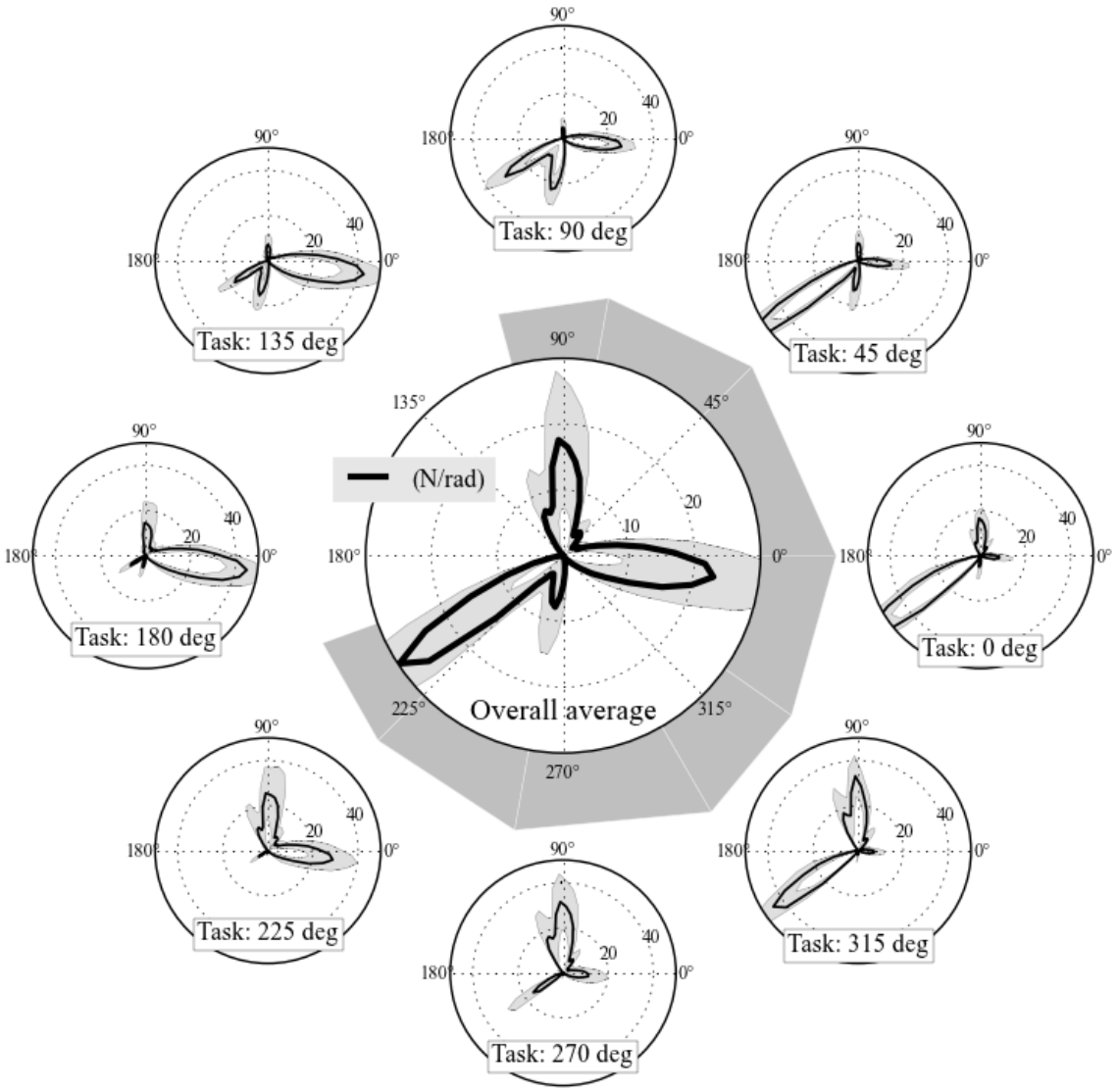

Figure 4 — Radial force distributions. Outside panels: averaged across subjects for each task direction. Central panel: averaged across subjects and directions, with a sketch of approximate hand posture. Error clouds depict standard deviations. The lighter patch is used for visual convenience to separate the thumb from the other phalanges.

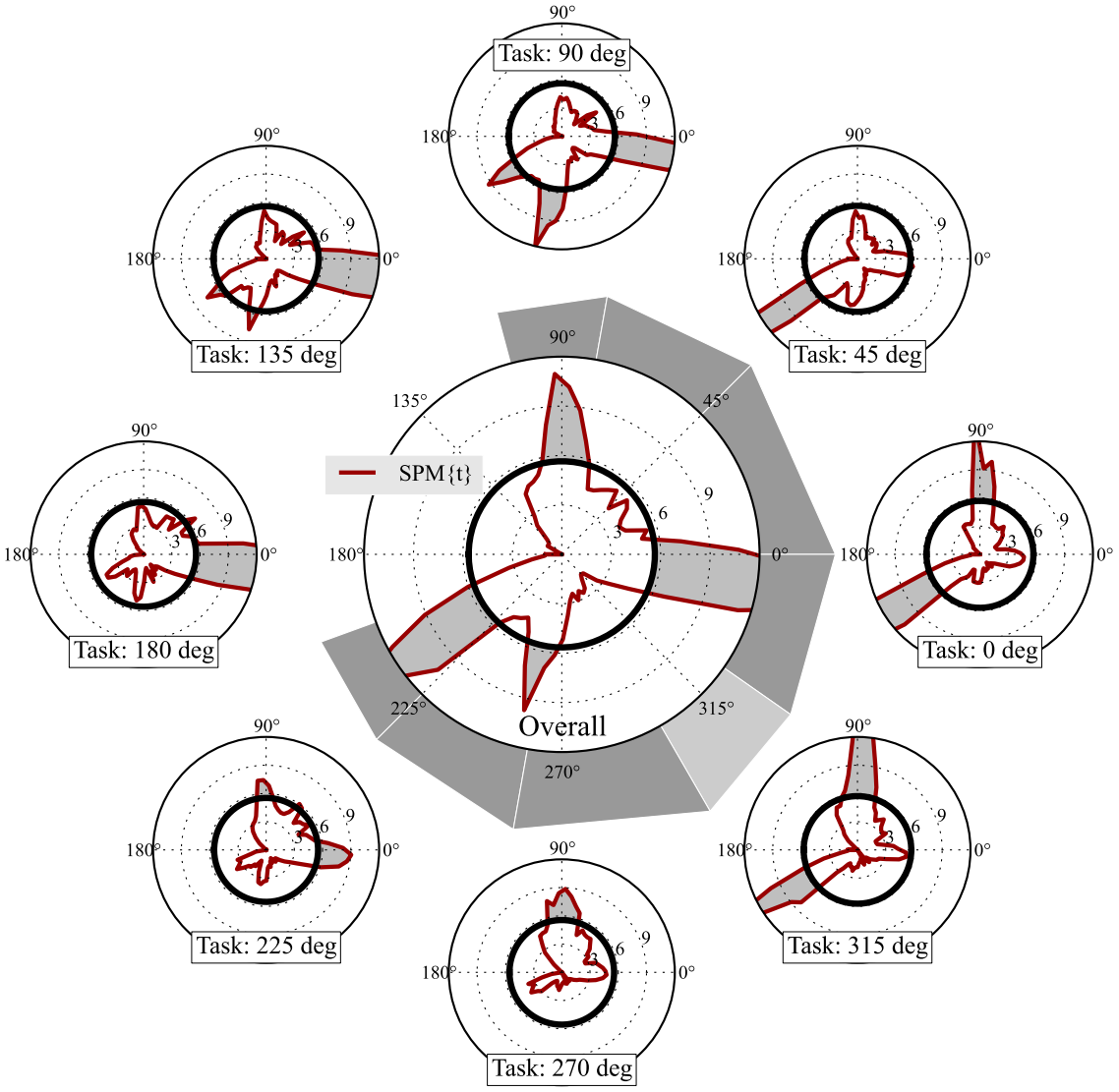

Figure 5 — Statistical parametric mapping (SPM) results. Outside panels: individual task directions. Central panel: all tasks combined, with a sketch of approximate hand posture. Data are *t* statistic distributions (SPM{t}), and represent the above mean trends normalized by their variances (Fig.4). Thick black rings depict the random-field-theory threshold for statistical significance ($t > 5.610$) at a family-wise error rate of α=0.05. Supra-threshold clusters are shaded for visual convenience.

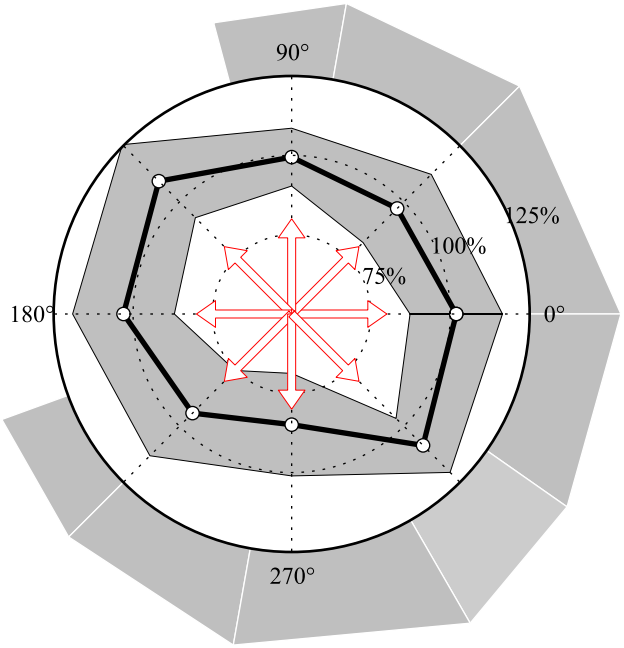

Figure 6 — Grasp force, that is: the force distribution integral, as a percentage of average within-subject grasp force across all tasks. Central arrows depict the task direction, and the hand sketch depicts the approximate posture. The error cloud depicts standard deviations.

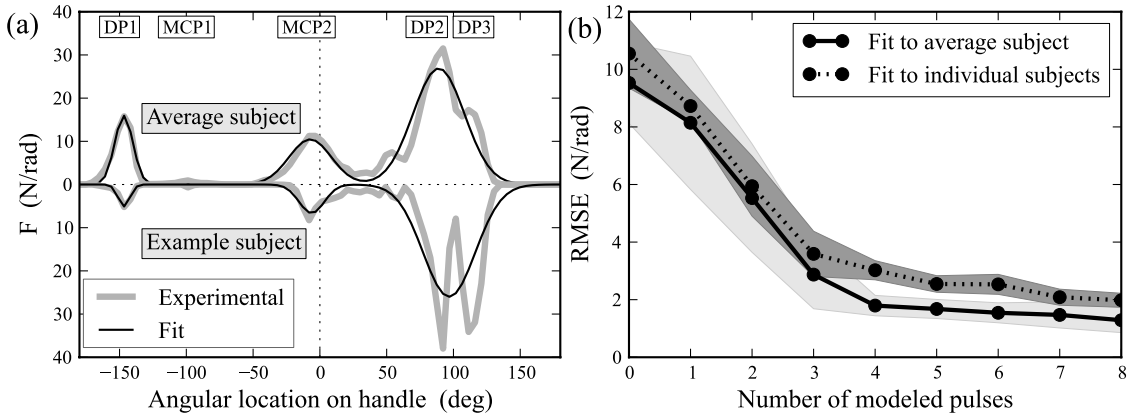

Figure 7 — (a) Example data fitting using three Gaussian pulses, task = -45°. The upper and lower panels depict the average subject and the subject from Fig.2, respectively. (b) Fitting error (root-mean-square error) as a the uniform distribution. Error clouds depict standard deviations.

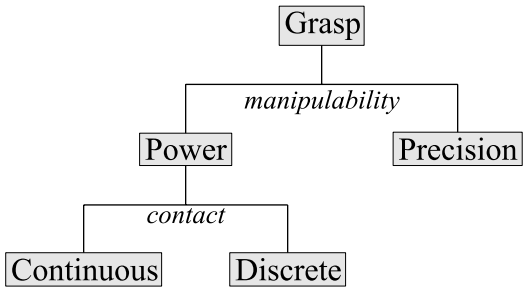

Figure 8 — Proposed revision to grasp taxonomy (c.f. Cutkosky and Wright, 1986). Power and precision grasps are distinguished only by manipulability, and power grasp contact areas can be continuous or discrete.